



Journal of Advanced Research in Fluid Mechanics and Thermal Sciences

Journal homepage:

https://semarakilmu.com.my/journals/index.php/fluid_mechanics_thermal_sciences/index

ISSN: 2289-7879



Characterization of Fluid Flow Through Porous Media

Nur Shamimi Amirah Md Sunhazim¹, Umami Aqila Norhaidi¹, Muhammad Afiq Witri Muhammad Yazid¹, Fazila Mohd Zawawi¹, Ummikalsom Abidin^{1,*}

¹ School of Mechanical Engineering, Faculty of Engineering, Universiti Teknologi Malaysia, 81310 Johor Bahru, Johor, Malaysia

ARTICLE INFO

Article history:

Received 20 February 2022

Received in revised form 13 May 2022

Accepted 18 May 2022

Available online 15 June 2022

Keywords:

Microfluidics; porous media; capillary flow; Lucas-Washburn equation

ABSTRACT

Microfluidic paper-based analytical devices (μ PADs) are highly in demand because of their important usage in the field of medical diagnostic, biology and environmental testing. Porous media has been used as a μ PADs with the benefits of cost-effective, excellent performance and ease of usage. Recently, porous media from paper-based filter paper has also been used as the main component for a self-powered imbibing micropump actuation. In this study, characterization of porous media from different specifications of Whatman ashless grade W40, W41 and W42 filter papers has been studied. In addition, the wicking or capillary flow capability of the porous media under an open and confined environment was also analyzed. Scanning Electron Microscope (SEM) and ImageJ image processing have been used as the method to determine the filter paper characteristics. Whatman filter paper grade W41 has the highest percentage of porosity which is 70.82 %. The porosity of filter paper grade W40 and W42 are 70.24 % and 61.8 % respectively. Meanwhile, experiments were conducted to understand the water wicking process for Whatman filter paper for different paper shapes and environments. Diamond-shaped filter paper resulted in faster wicking in the free environment compared with the constraint environment. The percentage difference of the wicking under these environments is 61.56 % and 141.09 % for W40 and W41 filter paper respectively. The experiment conducted also confirmed that the wicking behavior of the capillary height of the liquid in filter paper is proportional to the square root of the time. This result agreed well with the Lucas-Washburn equation. In conclusion, the characteristics of the liquid flow in porous media are closely related to its specification as provided by the manufacturer. Furthermore, the decrease of liquid wicking in a confined environment is the result of the high resistance of a liquid to flow with decreased filter paper porosity, permeability and thickness. This study provides important findings that will help in the optimization and best design of self-powered imbibing micropump for microfluidic device development.

1. Introduction

The last decade has seen a decrease in the size of devices while maintaining their purpose and increasing their functionality [1]. Microfluidic is one of the many technologies that is high in demand, which study the fluid movement and control in micro-scaled analysis. Microfluidic paper-based

* Corresponding author.

E-mail address: ummi@utm.my

<https://doi.org/10.37934/arfmts.96.2.2232>

analytical devices (μ PADs) are high in demand because progressively been used in medical diagnostic, biology and environmental testing. The benefits of μ PADs are cost-effective, excellent detection, user-friendly and potential for point-of-care (POC) diagnostic device that can be used outside health care facilities [2].

Reliance on the precise and predictable flow of liquids through the substrate is crucial for μ PADs. However, modelling the fluid's flow can be tricky since filter paper consists of randomly interwoven fibers of varying lengths and widths called complex porous media. Transport parameters in porous media flow are challenging because of its complex microstructures [3,4]. According to MacDonald [5], the porous media surface has multiple holes or porosity through which liquid particles flow. In many porous media application, liquid flow is enabled but solid particles retained as main characteristics of a filter paper. Past research on fluid flow through porous media especially on μ PADs still lacking on empirical evidence in understanding the physical mechanisms that affect the flow.

The main factors in determining the characterization of the fluid behaviour in the porous media are the porous materials, porosity and permeability [6,7]. Porosity is a critical parameter of porous medium in determining the materials' characteristics as it measures vacant space [8]. The porosity depends on porous media's fibre matrix structure. While the concept of porosity is simple and easy to understand, it blends many characteristics of the interfaces' shape and morphology. The factors responsible for pore morphology alterations are flow processes and the processes that strongly affect interfaces and influence those [9]. Another important factor is the permeability, which is the medium's ability to transport fluid [10]. There are many studies done, theoretically and experimentally, to determine the relation between permeability and other characteristics. According to the Eq. (1), it is concluded that the permeability is related to the porosity and specific surface of the porous medium [11,12].

$$k = \frac{p^3}{cS^2} \tag{1}$$

In this study, the characterization of the fluids flow through Whatman filter paper under a free and confined environment is studied experimentally and theoretically. The observation of SEM images using ImageJ processing is fulfilled to identify the porosity of the filter paper.

2. Methodology

2.1 Materials

Three different Whatman filter paper grades were used in this study which are filter paper grades 40, 41 and 42. Table 1 below shows the properties and description of each grade of filter paper taken from the Whatman catalogue. The filter papers are categorized with its capability in filtering solid particles where pore size is related to particle retention. Smallest pore size is also related to the slowest flow of fluid. Minimal or ashless filter papers are selected to reduce any ash interfering the fluid flow behavior.

Table 1
 Properties of Whatman filter paper

Grade	Description	Properties			
		Particle Retention (μm)	Typical Thickness (μm)	Basis Weight (g/m^2)	Ash Content (%)
W40	Medium Flow	8	210	95	0.007
W41	Fast Flow	20 – 25	220	85	0.007
W42	Slow Flow	2.5	180	100	0.007

2.2 ImageJ Processing

In obtaining the filter paper's porous media properties, the image processing step was essential for analyzing and manipulating the digital images. ImageJ is the image processing software used to identify porous media properties. This software provides user with a medium for scientific analysis of the image, particularly for microscopic inspection.

ImageJ is an image processing software for filter paper properties analysis. The microscopic images of the Whatman filter paper grade W40, W41 and W42 were obtained using scanning electron microscope (SEM). In the SEM sample preparation, the filter papers were cut into a circle-shaped of radius 1 cm. The SEM images were converted into digital images and analyzed using ImageJ. From the ImageJ analysis, the porosity of the filter papers was calculated. The image processing process is shown below in Figure 1.

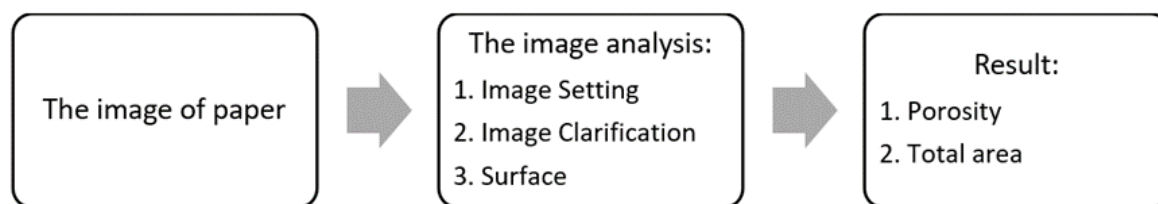


Fig. 1. The image processing process [13]

2.3 Experimental Study

For the experimental study, there are two different environments selected: free and confined environments. Each environment was tested with three different Whatman filter paper grades of W40, W41, and W42. There are also two different shapes used in the study which are rectangular and diamond shapes. In order to know the effect of volume on the fluid flow, two different sizes were chosen for rectangular shape. The detailed shapes and sizes are as listed below

- i. A1: small rectangular shape (A1): 7 mm × 25 mm
- ii. A2: big rectangular shape (A2): 7 mm × 50 mm
- iii. Diamond shape: (7 mm × 50 mm)

Figure 2 shows the setup of the wicking experiment set-up in an open space environment. Basically, there were four equipment used which are a digital camera for videotape the wicking liquid, the digital clock to measure the temperature and humidity of the open space surrounding, the petri dish to place the working liquid, and the stopwatch to time the filter paper to be fully absorbed with working liquid.



Fig. 2. The experimental setup in free environment

The images were observed at various time duration and were processed with InShot, an image and video editor. The wicking height was measured from the images regularly. The time taken for the paper strip to be fully absorbed from the first and second lines is also recorded. In the experiments, it is expected that the wicking behavior will strongly depend on grade of the paper strip and its specifications [14].

2.4 Theoretical Study

Constituent particles' sizes and pores remain fixed throughout the wicking process [15]. There are two conventional theories for wicking in rigid porous media: Darcy's Law, and Washburn equation (Lucas-Washburn equation). Masoodi *et al.*, [16] stated that Washburn's equation presumed the porous medium consists of a bundle of parallel capillary tubes of identical size. The wicking flow's central equation after deliberation of the Hagen-Poiseuille, fluids flow through such tubes and neglect the influence of gravity is in the Eq. (2)

$$\frac{4\gamma \cos(\theta)}{D_c} = \frac{32\mu L_{lf}}{D_h^2} \frac{dL_{lf}}{dt} \quad (2)$$

where; γ is fluid's surface tension, μ is fluid's viscosity, θ is contact angle, t is time, D_c is diameter of capillary pore, D_h is diameter of hydraulic pore, L_{lf} is height of the rising liquid-front.

The porous medium's porosity can be described as, the pore volume ratio to the total volume. p_c is the capillary pressure provided by the well-known Laplace Eq. (3)

$$p_c = \frac{2\gamma \cos(\theta)}{R_c} \quad (3)$$

3. Results

3.1 Scanning Electron Microscope (SEM) and ImageJ Analysis

Scanning electron microscope (SEM) is the common direct measurement method to study material microstructure [17]. The image captured from the SEM is then analysed using ImageJ to identify porous media properties [18]. In this study, the three Whatman filter paper of W40, W41

and W42 was observed under SEM and further analysed using ImageJ. Figure 3, Figure 4 and Figure 5 are SEM images before and after the threshold process using ImageJ.

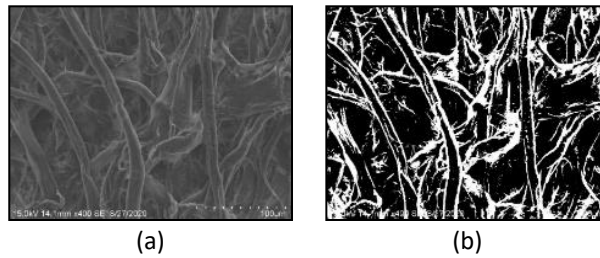


Fig. 3. SEM image grade W40. (a) Before threshold; (b) After threshold

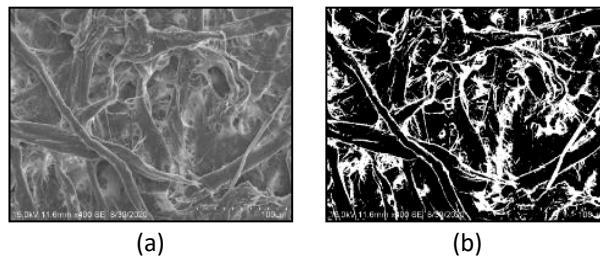


Fig. 4. SEM image grade W41. (a) Before threshold; (b) After threshold

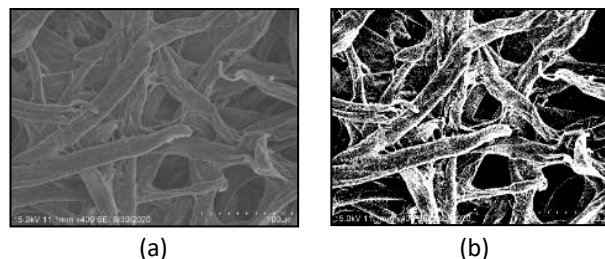


Fig. 5. SEM image grade W42. (a) Before threshold; (b) After threshold

The porosity of a filter paper has been assumed by Dal Dosso *et al.*, [19] to be 70% when the filter paper's size was constant. Cui *et al.*, [20] stated that the relationship between density and porosity is inverse because the lesser the pores, the faster the flow be able to be absorbed. Table 2 summarizes the results of the analysis porosity image of three images from ImageJ. The grade W41 has the highest percentage of porosity in the Table 2 of 70.82%. The highest porosity is because the total area of the paper is the largest when compared to the other two filter papers. It is possible to conclude that the filter papers' absorption rate is $W41 > W40 > W42$.

Table 2
 Summarization of Particle Analysis

Grade	Count	Total Area	Average Size	% Area	Mean
W40	1238	863049	697.13	70.24	255
W41	2104	870243	413.61	70.82	255
W42	11635	759337	65.26	61.80	255

3.2 Experimental Analysis

In the experimental study, the area of the A1 shape and diamond shape is the same, but the area of the A2 shape is not the same as the A1 shape and diamond shape. The similarities for all three shapes are the width which is 7 mm.

Figure 6 depicts a comparison of the time required for different areas of rectangular shape (A1 and A2) in a free environment. Based on the comparison, A1 shape takes less time to wholly absorbed than the A2 shape. This is due to the size of A2, which is twice the size of A1. The percentage difference in wicking for the various areas is 112.73% for W40, 99.53% for W41, and 119.31% for W42 filter paper. Nevertheless, both filter papers for grade 41 absorb completely the quickest, followed by grades W40 and W42 regardless of the size.

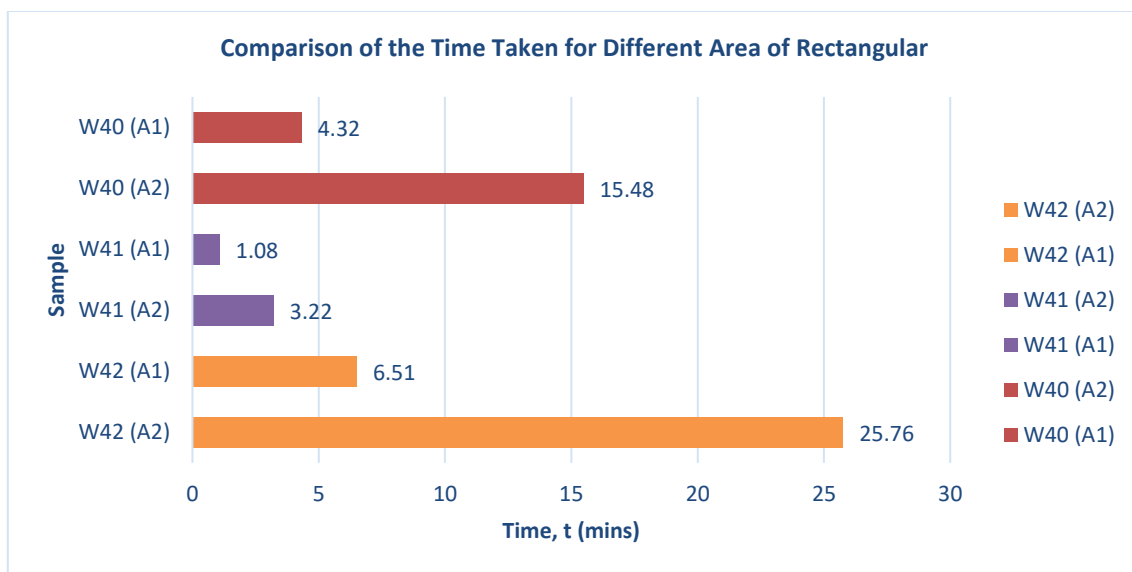


Fig. 6. Graph of Comparison of the Time Taken for Different Area of Rectangular

The diamond shape comprises two specular circular divisions that provide a steady flow in the first expanding element and a smooth transition to the end channel in the second restriction element [21]. A comparison of the time taken for different shapes in a free environment is displayed in Figure 7. From the result, the time taken for the A1 shape is quicker than the diamond shape. Sequentially, the wicking percentage difference for different shapes is 19.25 %, 1.83 %, and 46.91 % for W40, W41, and W42 filter paper.

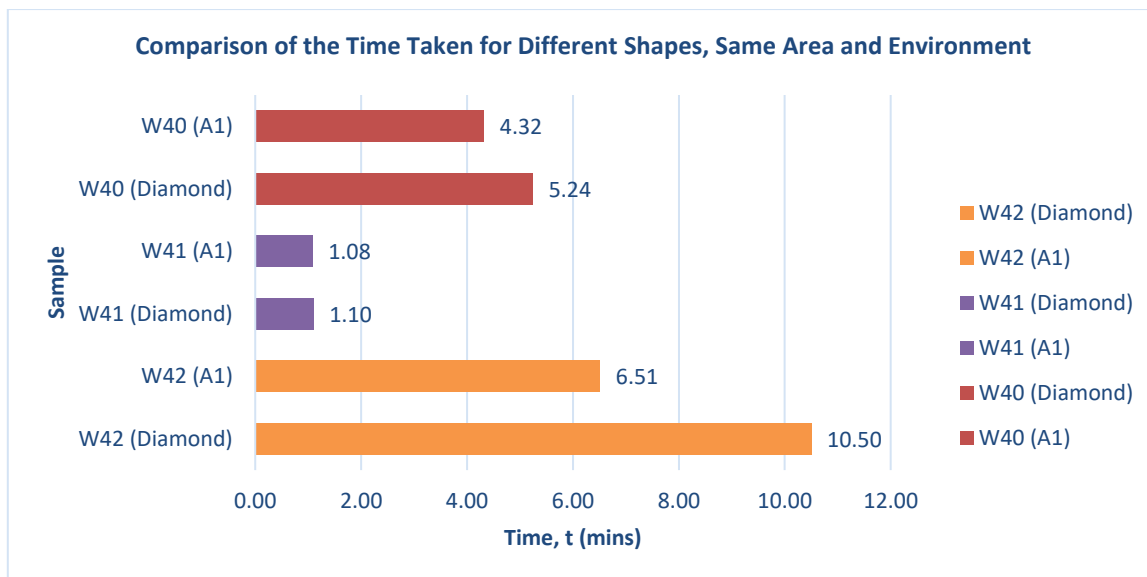


Fig. 7. Graph of Comparison of the Time Taken for Different Shapes, Same Area and Environment

Furthermore, the experimental study for the diamond shape was done in two different environments. The comparison of the time taken for different environments, same shapes, and areas is shown in Figure 8. Diamond shape filter paper resulted in faster wicking in the free environment compared with the confined environment. The percentage difference of the wicking under these environments is 61.56 % and 141.09 % for W40 and W41 filter paper respectively. This is due to the adhesive on the laminating film that is melted during laminating process and causes resistance for the fluid to flow inside the microchannel.

On the other hand, W41 took shorter time to absorb the liquid in both environments. This can be explained from the properties of the filter papers, which is the particle retention, which is the ideal diameter of the smallest particle blocked by the filter paper. This means that filter paper having smaller particles retention size will consist smaller volume of voids and have difficulty to absorb liquid. Thus, filter paper W41 took shorter time to absorb the water as it has bigger particle retention size than W40.

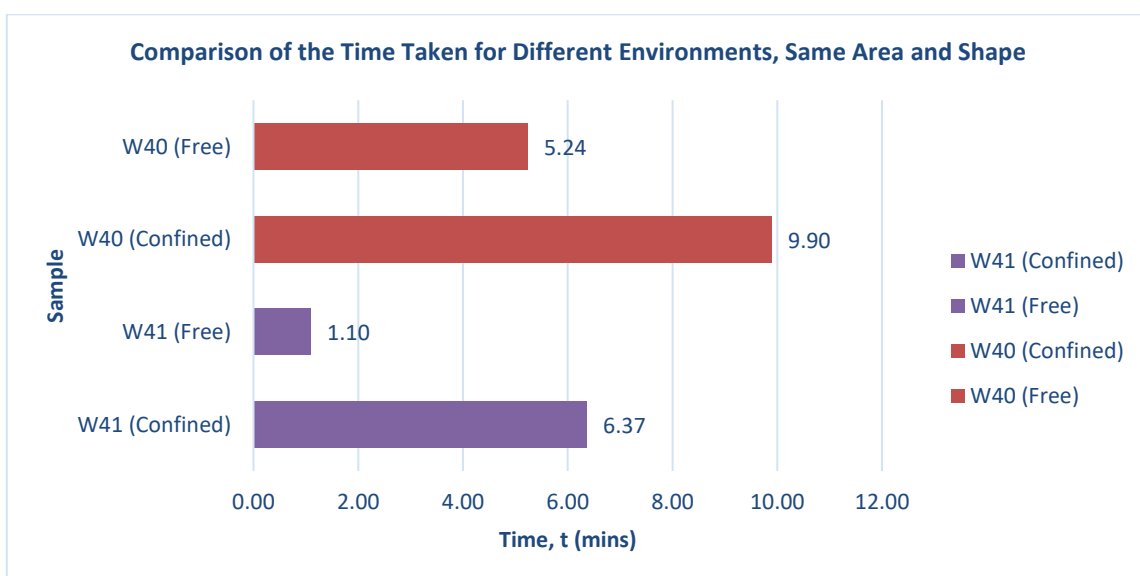


Fig. 8. Graph of Comparison of the Time Taken for Different Environments, Same Area and Shape

3.3 Theoretical Analysis

In a theoretical study, wettability and wicking are the two properties that lead to liquid flow in porous media. Wettability causes the porous surface to wet first, which allows the liquid to wick throughout the porous media. Wicking liquid happens instinctively in porous media because of the negative influence of capillary pressure [22]. However, according to Lucas Washburn's primary model of the wicking phenomenon, the paper comprises randomly oriented fibres, called paper bundles of capillary tubes [6]. Wicking is an event that happens during a dry porous material gets into contact with a fluid. The capillary forces precipitate the material to absorb the fluid. The absorption will absorb until the gravitational forces balance the capillary forces and equilibrium are achieved [23].

The flow rate along the filter paper can be simulated by the filter paper's length, permeability, and thickness [8]. Figure 9 describes a comparison of flow rates for various rectangular areas. Each of the filter papers used in this study has different properties. In this study, the factors affecting the flow rate are the filter paper's length and the thickness of the filter paper. The W41 grade filter paper flows the fastest due to the thickness, which is 220 μm , followed by W40 and W42. Moreover, it can also be concluded that the A1 shape filter paper has the highest flow rate compared to the A2 shape filter paper because the area of the A1 shape filter paper is smaller than the A2 shape filter paper.

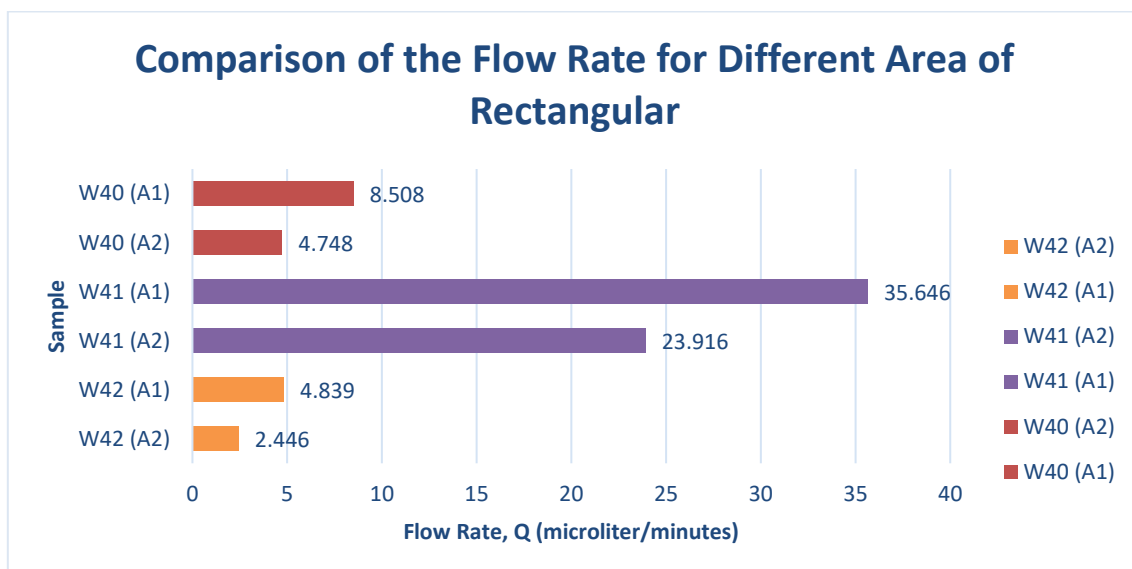


Fig. 9. Graph of Comparison of the Flow Rate for Different Area of Rectangular

Darcy's Law, in more detail, describes the equation that measures fluid flow through a porous medium. Based on the Figure 10, it can be concluded that W41 has the lowest pressure difference, followed by W40 and W42. Moreover, the pressure difference of the A2 shape filter paper is lower than the pressure difference of the A1 shape filter paper. This is because the area of the filter paper for A2 is bigger than A1. For W40, W41, and W42 filter paper, the percentage difference for pressure difference is 112.70 %, 99.61 %, and 109.28 %, respectively.

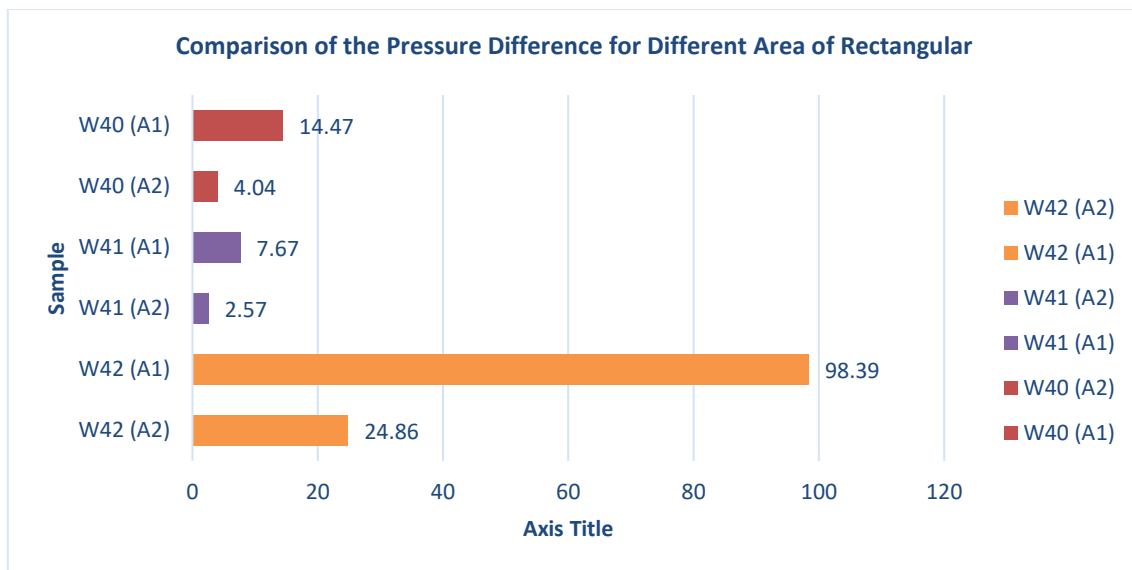


Fig. 10. Graph of Comparison of the Pressure Difference for Different Area of Rectangular

Figure 11 displays the comparison of the capillary rise of working fluid in paper strips as a function of time for various grades of filter paper. The bold colour of the line graph represents the experimental data while the lighter colour of the line graph represents the *L-W* model. In this study, the *L-W* model has a limitation in that it does not account for evaporation. Plus, the assumption of fluid flow in the circular capillary is as original *L-W*. The experimental capillary rise results were compared to the *L-W* model. The data of the experimental show almost similar results as the *L-W* model data.

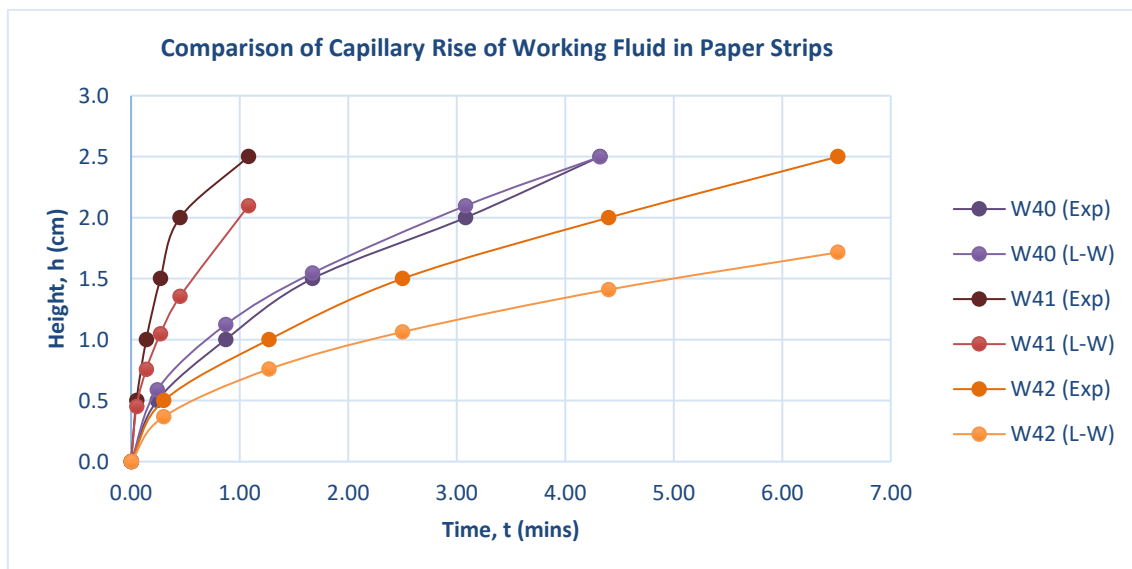


Fig. 11. Graph of the Comparison of Capillary Rise of Working Fluid in Paper Strips

From the comparison on experimental liquid wicking behavior and theoretical equation of *L-W*, a similar graphs trend was obtained. The highest wicking process was experienced by filter paper grade W40 and the lowest is from grade W42. Grade W42 demonstrated the slowest wicking due to its specification of slowest flow with smallest capillary radius and the least thickness. On the other hand, filter paper grade W41 has the fastest wicking due to its highest pore radius and categorized as fast flow from the manufacturer. The differences of the experimental and *L-W* also contributed with other

effect like evaporation of liquid to the surrounding environment. The evaporation model needs to be embedded in the L - W equation as mentioned in the work of Patari and Mahapatra [22]. In addition, Patari and Mahapatra [22] also recommended an improved capillary radius model in order to match correctly the experimental data and L - W equation. The new capillary radius equation proposed is

$$R_c = \frac{2\gamma\cos(\theta)}{\rho g L_{ss}} \quad (4)$$

where; R_c is particle radius, γ is liquid's surface tension, θ is contact angle, ρ is liquid's density, g is gravitational acceleration, L_{ss} is saturated capillary rise height.

4. Conclusions

In conclusion, this research successfully analysed the characterization of fluid flow through Whatman filter paper under a free and confined environment. Based on the SEM observations, image analysis and experiment, it can be concluded that filter paper with a higher porosity value would have higher particle retention and result in better water absorption. In this study, A1 shape takes less time to wholly absorbed than the A2 shape. This is due to the size of A1, which is twice less the size of A2. The percentage difference in wicking for the various areas is 112.73 % for W40, 99.53 % for W41, and 119.31% for W42 filter paper. Diamond-shaped filter paper resulted in faster wicking in the free environment compared with the constraint environment. The percentage difference of the wicking under these environments is 61.56 % and 141.09 % for W40 and W41 filter paper respectively. The experiment conducted also confirmed that the wicking behaviour of the capillary height of the liquid in filter paper is proportional to the square root of the time. For further analysis on the characterization of fluids flow, improvement and suggestions can be implemented. A digital cutter instead of cutting the filter paper manually by using a scissor or a pen knife. In addition, wide range of filter paper to be studied and analysed and experiment to be conducted in a control environment, Lastly, simulation using COMSOL Multiphysics software for wicking behaviour effect is suggested as future study.

Acknowledgement

This work was supported/funded by the Ministry of Higher Education under Fundamental Research Grant Scheme (FRGS/1/2019/TK03/UTM/02/2).

References

- [1] Jowsey, Mohamad Hafzan Mohamad, Natrah Kamaruzaman, and Mohsin Mohd Sies. "Heat and Flow Profile of Nanofluid Flow Inside Multilayer Microchannel Heat Sink." *Journal of Advanced Research in Micro and Nano Engineering* 4, no. 1 (2021): 1-9.
- [2] Mahmud, Md Almostasim, Eric J. M. Blondeel, Moufeed Kaddoura, and Brendan D. MacDonald. "Features in microfluidic paper-based devices made by laser cutting: How small can they be?." *Micromachines* 9, no. 5 (2018): 220. <https://doi.org/10.3390/mi9050220>
- [3] Roetting, Tobias, Luis Guarracino, Jesus Carrera, Linda Luquot, and Diosenia Casalnuovo. "A fractal model to describe the evolution of multiphase hydraulic properties during mineral dissolution." In *EGU General Assembly Conference Abstracts*, pp. EGU2013-8815. 2013.
- [4] Liu, Richeng, Bo Li, and Yujing Jiang. "A fractal model based on a new governing equation of fluid flow in fractures for characterizing hydraulic properties of rock fracture networks." *Computers and Geotechnics* 75 (2016): 57-68. <https://doi.org/10.1016/j.compgeo.2016.01.025>
- [5] MacDonald, Brendan D. "Flow of liquids through paper." *Journal of Fluid Mechanics* 852 (2018): 1-4. <https://doi.org/10.1017/jfm.2018.536>

- [6] Washburn, Edward W. "The dynamics of capillary flow." *Physical Review* 17, no. 3 (1921): 273-283. <https://doi.org/10.1103/PhysRev.17.273>
- [7] Fu, Elain, Stephen A. Ramsey, Peter Kauffman, Barry Lutz, and Paul Yager. "Transport in two-dimensional paper networks." *Microfluidics and Nanofluidics* 10, no. 1 (2011): 29-35. <https://doi.org/10.1007/s10404-010-0643-y>
- [8] Park, Juhwan, Joong Ho Shin, and Je-Kyun Park. "Experimental analysis of porosity and permeability in pressed paper." *Micromachines* 7, no. 3 (2016): 48. <https://doi.org/10.3390/mi7030048>
- [9] Gauvin, F., V. Caprai, Q. L. Yu, and H. J. H. Brouwers. "Effect of the morphology and pore structure of porous building materials on photocatalytic oxidation of air pollutants." *Applied Catalysis B: Environmental* 227 (2018): 123-131. <https://doi.org/10.1016/j.apcatb.2018.01.029>
- [10] Graczyk, Krzysztof M., and Maciej Matyka. "Predicting porosity, permeability, and tortuosity of porous media from images by deep learning." *Scientific Reports* 10, no. 1 (2020): 1-11. <https://doi.org/10.1038/s41598-020-78415-x>
- [11] Anovitz, Lawrence M., and David R. Cole. "Characterization and analysis of porosity and pore structures." *Reviews in Mineralogy and Geochemistry* 80, no. 1 (2015): 61-164. <https://doi.org/10.2138/rmg.2015.80.04>
- [12] Koponen, A., M. Kataja, and J. Timonen. "Permeability and effective porosity of porous media." *Physical Review E* 56, no. 3 (1997): 3319. <https://doi.org/10.1103/PhysRevE.56.3319>
- [13] Ihsani, Zadid. "Porosity Analysis Procedure with ImageJ." *Academia*. Accessed April 23, 2021. https://www.academia.edu/24152953/Porosity_Analysis_Procedure_with_ImageJ.
- [14] Liu, Zhi, Jie Hu, Yimeng Zhao, Zhiguo Qu, and Feng Xu. "Experimental and numerical studies on liquid wicking into filter papers for paper-based diagnostics." *Applied Thermal Engineering* 88 (2015): 280-287. <https://doi.org/10.1016/j.applthermaleng.2014.09.057>
- [15] Masoodi, Reza, and Krishna M. Pillai. "Darcy's law-based model for wicking in paper-like swelling porous media." *AIChE Journal* 56, no. 9 (2010): 2257-2267. <https://doi.org/10.1002/aic.12163>
- [16] Masoodi, Reza, Krishna M. Pillai, and Padma Prabodh Varanasi. "Role of hydraulic and capillary radii in improving the effectiveness of capillary model in wicking." In *Fluids Engineering Division Summer Meeting*, vol. 48401, pp. 251-259. 2008. <https://doi.org/10.1115/FEDSM2008-55172>
- [17] Zuhudi, Nurul Zuhairah Mahmud, Afiq Faizul Zulkifli, Muzafar Zulkifli, Ahmad Naim Ahmad Yahaya, Nurhayati Mohd Nur, and Khairul Dahri Mohd Aris. "Void and Moisture Content of Fiber Reinforced Composites." *Journal of Advanced Research in Fluid Mechanics and Thermal Sciences* 87, no. 3 (2021): 78-93. <https://doi.org/10.37934/arfmts.87.3.7893>
- [18] Rueden, Curtis T., Johannes Schindelin, Mark C. Hiner, Barry E. DeZonia, Alison E. Walter, Ellen T. Arena, and Kevin W. Eliceiri. "ImageJ2: ImageJ for the next generation of scientific image data." *BMC Bioinformatics* 18, no. 1 (2017): 1-26. <https://doi.org/10.1186/s12859-017-1934-z>
- [19] Dal Dosso, Francesco, Tadej Kokalj, Jaroslav Belotserkovsky, Dragana Spasic, and Jeroen Lammertyn. "Self-powered infusion microfluidic pump for ex vivo drug delivery." *Biomedical Microdevices* 20, no. 2 (2018): 1-11. <https://doi.org/10.1007/s10544-018-0289-1>
- [20] Cui, Zhiwei, Yongmin Huang, and Honglai Liu. "Predicting the mechanical properties of brittle porous materials with various porosity and pore sizes." *Journal of the Mechanical Behavior of Biomedical Materials* 71 (2017): 10-22. <https://doi.org/10.1016/j.jmbbm.2017.02.014>
- [21] Kokalj, Tadej, Younggeun Park, Matjaž Vencelj, Monika Jenko, and Luke P. Lee. "Self-powered imbibing microfluidic pump by liquid encapsulation: SIMPLE." *Lab on a Chip* 14, no. 22 (2014): 4329-4333. <https://doi.org/10.1039/C4LC00920G>
- [22] Patari, Subhashis, and Pallab Sinha Mahapatra. "Liquid wicking in a paper strip: An experimental and numerical study." *ACS Omega* 5, no. 36 (2020): 22931-22939. <https://doi.org/10.1021/acsomega.0c02407>
- [23] Masoodi, Reza, Krishna M. Pillai, and Padma P. Varanasi. "Effect of externally applied liquid pressure on wicking in paper wipes." *Journal of Engineered Fibers and Fabrics* 5, no. 3 (2010): 49-66. <https://doi.org/10.1177/155892501000500307>